Available online at www.sciencedirect.com
ScienceDirect
Applied Catalysis B: Environmental 79 (2008) 224–236
APPLIED CATALYSIS B: ENVIRONMENTAL
www.elsevier.com/locate/apcatb

Electro-Fenton and photocatalytic oxidation of phenyl-urea herbicides: An insight by liquid chromatography–electrospray ionization tandem mass spectrometry

I. Losito *, A. Amorisco, F. Palmisano

Centro Interdipartimentale di Ricerca S.M.A.R.T., c/o Dipartimento di Chimica, Università degli Studi di Bari, Via Orabona 4, 70126 Bari, Italy

Received 31 August 2007; received in revised form 25 October 2007; accepted 27 October 2007
Available online 4 November 2007

Dedicated to Prof. Pier Giorgio Zambonin on the occasion of his 72nd birthday.

Abstract

The degradation pathways exhibited by three phenyl-urea herbicides: isoproturon (ISO), chlortoluron (CHLT) and chloroxuron (CHLOX), during photocatalytic (on supported TiO_2 under intense solar radiation) and electro-Fenton (EF) treatment were investigated by HPLC coupled to electrospray ionization single and tandem mass spectrometry (HPLC–ESI-MS and MS/MS). In particular, the dependence of degradation efficiency on the initial concentration ratio between substrate and Fe(III) ion was assessed for the EF treatment and a 1:1 ratio was found to be optimal. A comparison between photocatalytic and EF degradation, in terms of structures, number and evolution on a similar time scale (up to 5 h) of by-products, was then performed. Similar reactivities were found in the two cases, hydroxylation (single and multiple, with H, alkyl groups or Cl substitution, depending on the herbicide) and demethylation on the dimethylamino moiety (eventually followed by hydroxylation) being the most relevant processes in by-products generation. The scale of EF degradation efficiency for the three herbicides was almost identical to the photocatalytic one (ISO > CHLT ≈ CHLOX), yet electro-Fenton proved to be a more efficient process, generally leading to a faster further degradation of by-products.

Keywords: Phenyl-urea herbicides; Electro-Fenton degradation; Photocatalytic degradation; Liquid chromatography–electrospray ionization mass spectrometry

1. Introduction

Phenyl- and sulfonyl-urea derivatives are widely adopted as selective pre- and post-emergence herbicides for the control of most broad-leaved weeds and annual grasses in many agricultural crops. In spite of their high herbicidal activity, low application rates (10–40 g ha^{-1}) and low toxicity to mammals, the use of urea herbicides is not without tradeoffs. Indeed these compounds could act as persistent water pollutants due to their fairly high water solubility and relative photochemical stability. Recent environmental monitoring studies [1–3] indicated chlortoluron, linuron and isoproturon as the herbicides detected with greatest frequency in surface and ground water samples collected in agricultural areas.

As a consequence, different strategies have been devised for the removal of these pollutants from water. Among them, advanced oxidation processes (AOPs) [4,5] have received great attention in the last two decades. In particular, photocatalytic processes [6], in which generation of reactive $^{\bullet}OH$ radicals is mediated by inorganic semiconductors exposed to UV–vis radiation (e.g. TiO_2 exposed to radiation with $\lambda \leq 354$ nm) have been thoroughly investigated. Methods based on photocatalysis using either TiO_2 suspensions [7–10] or TiO_2 supported on an inert substrate [11–13] have been studied for phenyl-urea degradation.

Among the latter, a new approach for TiO_2 immobilisation on glass, based on the use of a UV-transparent polymer, polyvinylidenefluoride (PVDF), as entrapping membrane has been recently developed in our laboratory [14], as part of a more general investigation on pollutants degradation strategies. The resulting TiO_2/PVDF composite has been then applied to the photodegradation (under artificial UV and/or solar

* Corresponding author.
E-mail address: losito@chimica.uniba.it (I. Losito).

0926-3373/$ – see front matter © 2007 Elsevier B.V. All rights reserved.
doi:10.1016/j.apcatb.2007.10.029

irradiation) of important phenyl-urea pesticides such as isoproturon [15], chlortoluron and chloroxuron [16] and several degradation by-products have been identified by liquid chromatography–electrospray ionisation–tandem mass spectrometry (LC–ESI–MS/MS).

Within this investigation, another promising method for pollutants degradation has been taken into consideration, the so-called *electro-Fenton* process. Actually the use of the Fenton reagent in AOPs for organic compounds of environmental concern dates back to the beginning of 1990s [17,18]. In this case $^{\bullet}OH$ radicals are generated by the following reaction:

$$Fe^{2+} + H_2O_2 \rightarrow Fe^{3+} + OH^- + {}^{\bullet}OH \quad (1)$$

As the disposal of ferric hydroxide sludge is one of the major drawbacks of ordinary Fenton process, the corresponding electrochemical variant (electro-Fenton, EF) has been proposed as an alternative degradation strategy [19]. In the EF process the Fenton's reagent is electrogenerated *in situ* at the cathode of an undivided cell containing an acidic solution fed with air or oxygen.

In particular H_2O_2 is generated according to the following reaction:

$$O_{2(g)} + 2H^+ + 2e^- \rightarrow H_2O_2 \quad (2)$$

at different electrodes, such as reticulated vitreous carbon, mercury pool, carbon-felt and O_2-diffusion cathodes [20–23]. The simultaneous generation of Fe^{2+} ions at the cathode is triggered by ferric ions added to the electrolytic solution in catalytic amounts, according to the following reaction:

$$Fe^{3+} + e^- \rightarrow Fe^{2+} \quad (3)$$

Cathodic reactions (2) + (3) provide reagents for the Fenton process (see reaction (1)) occurring in homogeneous solution. Catalytic reaction (1) is propagated from Fe^{2+} regeneration, through reaction (3) and *via* other processes involving Fe^{3+} species and (i) H_2O_2 (reaction (4)); (ii) organic radical intermediates $R^{\bullet}$ (reaction (5)) and (iii) hydroperoxyl radicals $HO_2^{\bullet}$ (reaction (6)), previously formed through reaction (4):

$$Fe^{3+} + H_2O_2 \rightarrow Fe^{2+} + HO_2^{\bullet} + H^+ \quad (4)$$

$$Fe^{3+} + R^{\bullet} \rightarrow Fe^{2+} + R^+ \quad (5)$$

$$Fe^{3+} + HO_2^{\bullet} \rightarrow Fe^{2+} + H^+ + O_2 \quad (6)$$

The anodic process is maintained by water oxidation at a platinum or stainless steel anode. Recently, boron-doped diamond (BDD) electrodes have been also adopted successfully as anodes [24,25].

In a variant of the EF process, the so-called photo-electro-Fenton (PEF) process, UV irradiation has been also used to improve the degradation efficiency [26,27]. The latter has been calculated for EF and/or PEF processes on a number of pollutants including atrazine [28], 4-chloro-2-methylphenol [27], azo dyes [29], 3,6-dichloro-2-methoxybenzoic acid [26], chlorophenoxy herbicides [30–32], pentachlorophenol [33] and aniline [34].

Recently, the EF degradation of the diphenylurea antimicrobial *triclocarban* in a CH_3CN/H_2O mixture has been reported [35], yet, to the best of our knowledge, neither EF nor PEF degradation of phenyl-urea herbicides have been attempted so far.

In this paper the three herbicides already considered as model compounds for TiO_2-based photocatalytic degradation of phenyl-ureas, namely *isoproturon*, *chlortoluron* and *chloroxuron*, have been subjected to electro-Fenton degradation under different conditions:

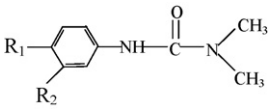

	R_1	R_2
Isoproturon	$(CH_3)_2CH$	H
Chlortoluron	CH_3	Cl
Chloroxuron	*p*-ClC_6H_4O	H

In particular, the best herbicide/Fe(III) concentration ratio, in terms of herbicide degradation rate, has been evaluated preliminarily. Afterwards, the by-product structures and kinetics have been studied by LC–ESI-MS and MS/MS and a comparison has been made with the corresponding data arising from photocatalysis on supported TiO_2 under intense solar irradiation.

2. Experimental

2.1. Materials

Herbicides standards: isoproturon or 3-(4-isopropylphenyl)-1,1-dimethylurea, CAS RN [34123-59-6]; chlortoluron or 3-(3-chloro-*p*-tolyl)-1,1-dimethylurea, CAS RN [15545-48-9]; chloroxuron or *N*-[4-(4-chlorophenoxy)phenyl]-*N*,*N*-dimethylurea, CAS RN [1982-47-4] were obtained from Dr. Ehrenstorfer (Augsburg, Germany). Stock solutions of each herbicide were prepared in acetonitrile at 1000 mg L^{-1}. Standard solutions and mixtures were prepared by dilution of the stock solutions with HPLC-grade water. HPLC gradient-grade acetonitrile (CH_3CN) and acetic acid (CH_3COOH) were purchased from Carlo Erba (Milan, Italy); LC grade water was from Fluka Chemika (Buchs, Switzerland).

Fe(III) sulfate, used as source of ferric ions during the electro-Fenton process, and ammonium acetate, used as additive in HPLC separations, were purchased from Sigma–Aldrich (Milan, Italy).

2.2. Equipment and procedures

2.2.1. Electro-Fenton

Electro-Fenton experiments were carried out in a three-electrode undivided electrochemical cell (EG&G) controlled by a potentiostat–galvanostat Model 273A (EG&G). The working electrode was a reticulated vitreous carbon (RVC) sponge (80 pores per linear inch) purchased from Le Carbone

Lorraine (La Défense Cedex, France), which was cut as a rod having a square section (1 cm × 1 cm) and a 5 cm length. During electro-Fenton degradations the rod was fixed to a cylindrical steel support (used for the electrical contact) through a metal clamp and then immersed vertically into the electrolytic solution up to a 1 cm length, in order to have a RVC volume of 1 cm^3 exposed to the solution. Based on the manufacturer's indications on the RVC surface area, this volume corresponds to an electrode area of 55 cm^2. The counter electrode was a (2.5 cm × 2.5 cm) platinum sheet; a Ag/AgCl, 3 M Cl^- was used as the reference electrode.

Electrolyses were performed potentiostatically at a −0.5 V potential, as already reported in the literature [33], in aerated herbicide solutions (total volume 50 mL, herbicide concentration 5 mg/L) under magnetic stirring. A catalytic quantity of ferric ion was introduced in the solution before the beginning of electrolysis by adding a small volume of a 10^{-2} M Fe^{3+} solution (according to the substrate/ferric ion concentration ratio investigated) to a 10^{-2} M H_2SO_4 solution.

The electrolytic solution pH was constantly monitored during the process and, if necessary, readjusted to values around 3 by dropwise addition of 10^{-2} M H_2SO_4.

One hundred microliter aliquots were withdrawn at regular time intervals within a 5–6 h time range and analysed by reverse-phase liquid chromatography–electrospray ionization-mass spectrometry.

2.2.2. Photocatalysis on supported TiO_2

Photocatalytic degradations were performed by exposing herbicide solutions (at the same initial concentrations as those adopted for EF treatments) to solar radiation in the presence of a composite PVDF-TiO_2 film (deposited on a glass slide), according to the already reported procedure [15,16].

In order to exploit the maximum solar radiation intensity possible, photocatalytic experiments were performed over a 5 h time interval, between 10 a.m. and 3 p.m., only during days with clear sky in June 2007. Integrated daily solar radiation energy at sea level in the same days ranged between 24,000 and 29,000 kJ m^{-2} (data provided by the National Agro-Meteorological Database of UCEA, Internet site: www.ucea.it), corresponding to the highest values of the year in Bari.

Similarly to EF, 100 μL aliquots of photocatalytically degraded herbicide solutions were periodically withdrawn and subjected to HPLC–ESI-MS,MS/MS analysis.

2.2.3. HPLC–UV–ESI-MS

The HPLC system consisted of a Waters (Mildford, MA, USA) 600-MS quaternary solvent pump connected to a Supelcosil LC-8-DB or LC-18-DB (according to the analysed herbicide) analytical column (250 mm × 2.1 mm i.d., particle diameter 5 μm, purchased from Supelco, Bellefonte, PA, USA).

A UV–vis variable wavelength detector (Agilent 1100) was directly connected to the HPLC column and operated at λ = 240 nm for a first monitoring of eluted species.

The outlet of the UV–vis detector was introduced into a LCQ ion trap mass spectrometer (ThermoElectron Corp., San Jose, CA, USA) through its electrospray ionization interface (ESI). It is worth noting that in the case of samples obtained from EF experiments the connection of the UV detector outlet to the LCQ ESI interface was delayed by 4 min, in order to minimise the introduction of Fe ions (eluted from C8/C18 columns in the dead volume) into the mass spectrometer.

The six-port Rheodyne valve (30 μL injection loop) of the LCQ instrument was used as chromatographic injector.

2.3. HPLC and ESI-MS conditions

HPLC separations were accomplished at 0.2 mL min^{-1} flow rate, using a binary gradient elution. The mobile phase consisted of 50 mM ammonium acetate solution in water: solvent A, and methanol: solvent B.

Different elution programs and/or stationary phases were found to be optimal for the HPLC separation of the three herbicides from their by-products: isoproturon (linear from 20 to 80% solvent B in 35 min, C8 column); chlortoluron (linear from 10 to 90% solvent B in 37 min, C18 column); chloroxuron (linear from 10 to 90% solvent B in 20 min, isocratic at 90% solvent B for 5 min, C8 column). In all cases, the return to initial mobile phase composition occurred in 2 min and was followed by a 13 min equilibration time.

MS data were acquired in the positive ion mode using the Xcalibur (ThermoElectron) software. Values adopted for the ESI interface and ion optics parameters and conditions for MS *full scan*, MS-*Selected Ion Monitoring* (SIM) and MS–MS *full scan* acquisitions have been already reported [15,16].

In the following, and also in the figures and schemes of this work, herbicide by-products will be shortly referred to by the *m/z* ratio of the protonated $[M + H]^+$ molecular ion.

3. Results and discussion

3.1. Effect of Fe^{3+} concentration on herbicide degradation

As the substrate/Fe(III) ion concentration ratio is a crucial issue in Fenton processes [27], the degradation kinetics of the target phenyl-urea herbicides were investigated at different [substrate]/[Fe^{3+}] ratios, namely 1, 2 and 10.

The peak areas (*A*) calculated from the HPLC–ESI-MS traces (SIM mode) relevant to each herbicide solution at different degradation times, normalised to that at $t = 0$ (A_t/A_0), were used to estimate the herbicide concentration. Data relative to isoproturon (ISO) are reported in Fig. 1 and compared to those observed in a parallel experiment for isoproturon photocatalytic degradation on supported TiO_2 under intense solar irradiation.

For the sake of comparison, curves arising from data interpolation using pseudo-first-order kinetics are also shown in the figure.

As can be seen, at [ISO]/[Fe^{3+}] = 10 a relatively low degradation rate (kinetic constant: 9.4×10^{-3} min^{-1}) was observed for the EF process, 90% removal of the herbicide being observed only after 5 h. A remarkable improvement in degradation efficiencies was observed for [ISO]/[Fe^{3+}] ratios

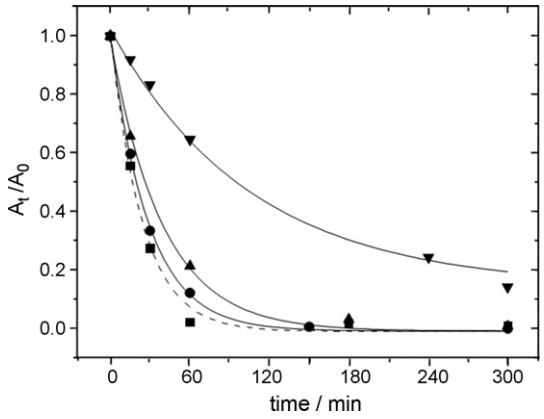

Fig. 1. Normalised (to time 0) peak areas vs. time plot for isoproturon (ISO) degradation by electro-Fenton (at different [ISO]/[Fe^{3+}] ratios) and TiO_2 photocatalytic process under solar irradiation. Initial ISO concentration C_0 = 24 μM. Curves correspond to interpolations based on pseudo-first-order kinetics (see text for details). Photocatalytic data are reported as (▲), EF data as: (■) ([ISO]/[Fe^{3+}] 1:1), (●) ([ISO]/[Fe^{3+}] 2:1) and (▼) ([ISO]/[Fe^{3+}] 10:1).

1:1 and 2:1 (kinetic constants: 4.2×10^{-2} and 3.4×10^{-2} min^{-1}, respectively), which led to a nearly complete removal of isoproturon after 1 h electrolysis. The corresponding kinetics were almost comparable to those observed, in the best conditions (i.e. sunny days in June), for photocatalysis on supported TiO_2 (kinetic constant: 2.6×10^{-2} min^{-1}). However, photocatalytic experiments performed in less favourable conditions (e.g. sunny days in December or January, when daily solar radiation energies can be even five times lower than those registered in summer) provided half-life times up to 100 min, values comparable to the worst ones obtained in this work by the EF treatment (see Fig. 1).

The results obtained in a recent investigation [35] on the EF degradation of *triclosan* (2,4,4-trichloro-2-hydroxydiphenyl-ether) in a Pt/carbon-felt cell, under conditions similar to those applied in the present work (although a galvanostatic approach was adopted in that case), can help in interpreting the observed dependence of EF efficiency on the [ISO]/[Fe^{3+}] ratio.

In fact, a rapid increase of Fe^{2+} concentration, up to a total conversion of the initial Fe^{3+} (0.2 mM), was observed when using a Pt/carbon-felt cell [35], with H_2O_2 concentration reaching similar values at its maximum. As the final $^{\bullet}OH$ radicals concentration, and then the degradation efficiency, is strictly related to that of Fe^{2+} ions (see reaction (1)), the initial [Fe^{3+}] values play a key, though indirect, role in determining the process kinetics in systems involving carbon cathodes (a very different scenario is observed when O_2 diffusion cathodes are used [35]).

It is then not surprising that the degradation efficiency for isoproturon is increased when the [Substrate]/[Fe^{3+}] ratio is decreased, i.e. when the concentration of Fe^{3+} becomes higher (being the concentration of substrate fixed).

Tests for electro-Fenton degradation at the same [ISO]/[Fe^{3+}] ratios were performed also on chlortoluron (CHLT) and chloroxuron (CHLOX). Again, the 1:1 [Substrate]/[Fe^{3+}] ratio was found to be the optimal one.

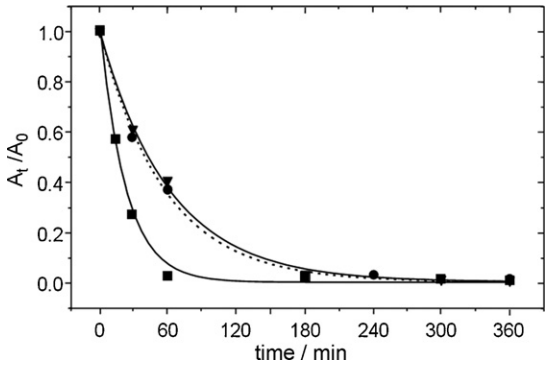

Fig. 2. Herbicide normalised (to time 0) peak areas vs. time plots during EF process performed at [Fe^{3+}]/[herbicide] = 1. Initial concentrations: [ISO] = 24 μM; [CHLT] = 23 μM; [CHLOX] = 17 μM. Curves correspond to interpolations based on pseudo-first-order kinetics (see text for details). (■) Isoproturon; (▼) chloroxuron; (●) chlortoluron (dotted line).

In Fig. 2 the time evolutions of chlorinated substrates concentrations (normalised to the initial values) are compared to those observed for ISO in the same conditions. The data could be fitted successfully using a pseudo-first-order kinetic model and the following values (expressed as min^{-1}) were obtained for the kinetic constants—ISO: 4.2×10^{-2}; CHLOX: 1.6×10^{-2}; CHLT: 1.7×10^{-2}.

The two chlorinated herbicides are clearly more refractory to EF degradation than isoproturon, whereas the respective degradation rates are almost comparable. This evidence is in accordance with data obtained during photocatalysis in the optimal conditions [16].

It is also interesting to note that the kinetic constants obtained in the present investigation are about an order of magnitude lower than those observed for triclosan in Ref. [35]. This difference is in agreement with that of initial [Fe^{3+}] concentrations adopted in the two cases (0.017–0.024 vs. 0.2 mM).

The decrease of precursor concentration can provide useful kinetic information, yet it is just one of the crucial points in establishing the real efficiency of a degradation strategy. Information on the by-products evolution is important as well, since many of them can be even more toxic than the precursors.

A characterisation of the phenyl-urea by-products obtained by the EF process in the best conditions ([Substrate]/[Fe^{3+}] = 1) was then undertaken starting from MS and MS/MS data acquired during HPLC separations and a comparison was made with data relevant to photocatalytic degradation.

3.2. Isoproturon degradation pathway

The total ion chromatogram (TIC) obtained in MS *full scan* mode on an aliquot of the electro-Fenton reaction mixture for isoproturon (ISO initial concentration: 5 mg/L or 2.4×10^{-5} M, reaction time 1 h) is shown in Fig. 3. Besides the herbicide peak at least six by-products are apparent in the TIC trace: one species with *m/z* 193, three species with *m/z* 223 and two species with *m/z* 239. These, however, are just a part of all the by-products observed for ISO by the adopted LC–MS analysis.

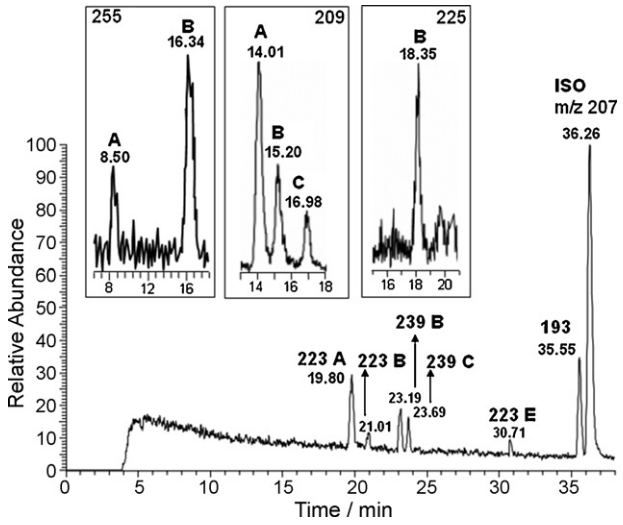

Fig. 3. Total ion current chromatogram (MS *full scan* acquisition mode) obtained after 1 h of EF degradation on an ISO 24 μM solution. EF conditions as specified in Section 2. Each chromatographic peak is marked with the *m/z* value of the corresponding $[M + H]^+$ ion and, where necessary, with a letter, corresponding to a specific isomer (see Ref. [15] for the nomenclature). In the insets: detailed view of extracted ion chromatograms for *m/z* 255, 209 and 225.

Indeed, extraction of ion currents on specific *m/z* ratios, calculated for further potential by-products (e.g. those observed for ISO during photocatalytic degradation), revealed the additional presence of three species at *m/z* 209, one species at *m/z* 225 and two species with *m/z* 255. Details of the corresponding extracted ion chromatograms are provided in the three insets of Fig. 3.

Moreover, two weak further peaks, corresponding to those observed for compounds 239A and D in Ref. [15], were observed in the extracted ion chromatogram for the *m/z* 239 ion (not shown).

It is worth noting that all the reported values were also found in the HPLC–ESI-MS and MS/MS investigation on isoproturon photocatalytic degradation by-products. Actually, the interpretation of the relevant MS/MS data in terms of molecular structure lead to identify most EF by-products as identical to photocatalytic ones [15], as explained in Table 1 and shown in Schemes 1 and 2. Nonetheless, as apparent from Table 1, some remarkable differences in the number of by-products observed for a particular *m/z* ratio were found.

First, the species at *m/z* 181, previously identified [15] as an ISO derivative in which the isopropyl group has been replaced by a OH group, is absent in the EF process. Moreover, two mono-hydroxylated isomeric species, classified as 223C and D in the previous work [15] (in Refs. [15,16] the letters were adopted to indicate the succession of by-products in terms of chromatographic retention times) are lacking, whereas an additional isomeric species at *m/z* 209 is formed in the EF process.

Table 1
Comparison between type and number of by-products observed during degradation of isoproturon (ISO), chlortoluron (CHLT) and chloroxuron (CHLOX) by immobilised-TiO_2 photocatalysis under solar irradiation (Phot.) and electro-Fenton (EF) processes

By-product	ISO			CHLT			CHLOX		
	m/z	Phot.	EF	m/z	Phot.	EF	m/z	Phot.	EF
Monohydroxylated	**223**	5	3	**229**	4	2	**307**	3	3
Bi-hydroxylated	**239**	4	4	**245**	4	3			
Tri-hydroxylated	**255**	2	2	**261**	--	1			
Demethylated on the dimethylaminic moiety (CH_3/H substitution)	**193**	1	1	**199**	1	1	**277**	1	1
Demethylated/hydroxylated on the dimethylaminic moiety	**209**	1	2						
Demethylated on the isopropyl group/hydroxylated (CH_3/OH substitution)	**209**	1	1						
Demethylated/bi-hydroxylated	**225**	2	1						
Isopropyl substituted by OH	**181**	1	--						
Demethylated on the benzene ring/hydroxylated (CH_3/OH substitution)				**215**	1	--			
Dechlorinated (Cl/H substitution)				**179**	1	1			
Chlorinated				**247**	--	2			
Dechlorinated/bi-hydroxylated							**289**	2	2
4-Cl-phenoxyl replaced by OH							**181**	1	1
Demethylated and with 4-Cl-phenoxyl replaced by OH							**167**	1	1
Dechlorinated/hydroxylated				**195**	1	--	**273**	1	1

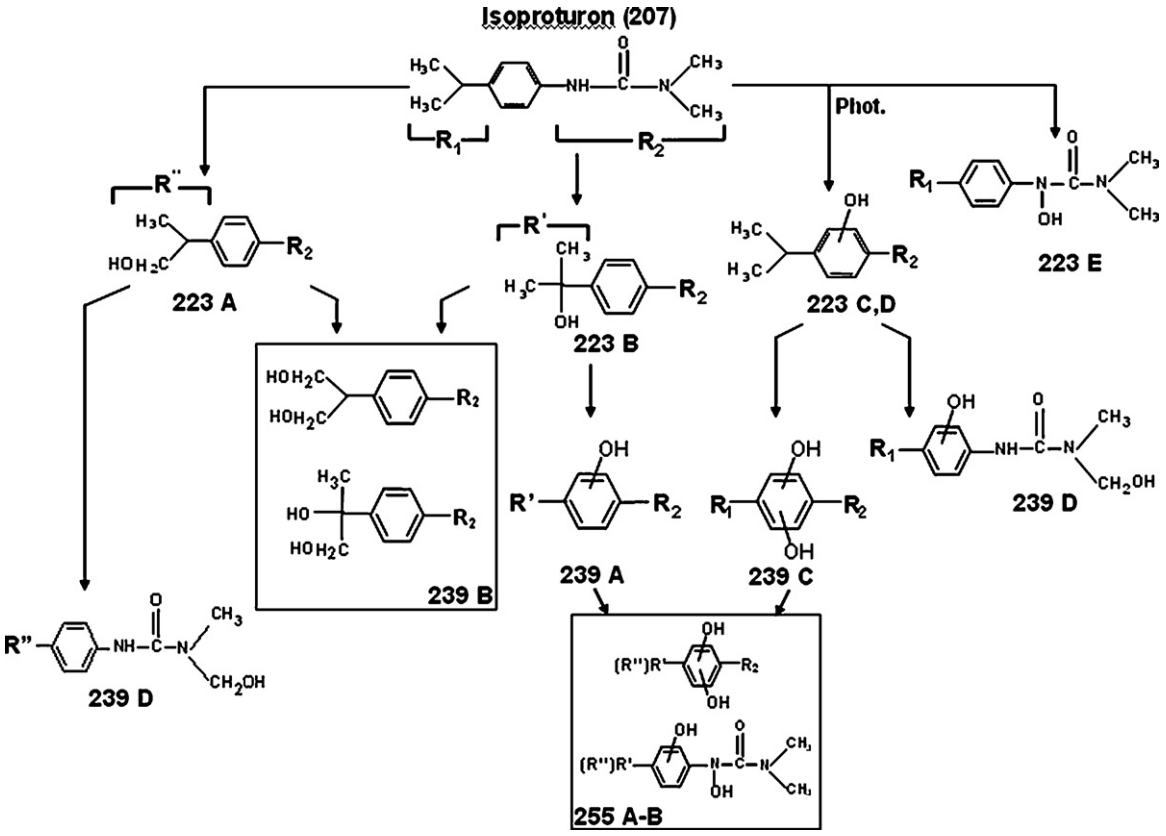

Scheme 1.

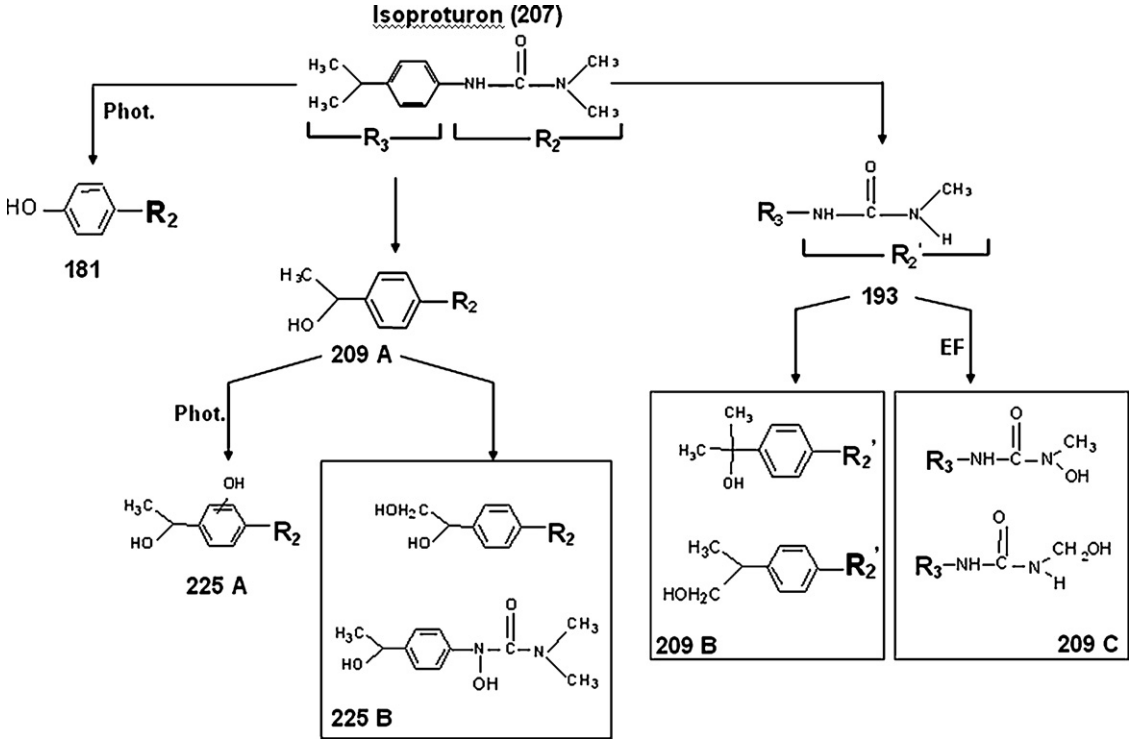

Scheme 2.

As for the last species (peak C in the corresponding inset to Fig. 3), the fragment at *m/z* 72, previously found as diagnostic of an intact dimethylaminic moiety on the precursor ion of phenyl-ureas [15,16], was lacking in the corresponding MS/MS spectrum.

The presence of two main fragments: (i) *m/z* 134, explained by the following structure:

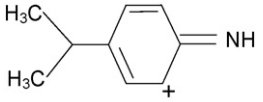

and (ii) *m/z* 191, arising from water loss, lead to suggest two possible structures for 209C – see Scheme 2 – corresponding to hydroxylation either directly on the N(1) or on the remaining N-linked methyl group of demethylated isoproturon (*m/z* 193).

The time evolutions of the most representative intermediates of ISO degradation observed during photocatalysis and EF processes, evaluated from the corresponding HPLC–ESI-MS SIM peak areas, are compared in Fig. 4. For the sake of clarity, only data for the most abundant species are reported for each class of isomers.

It is worth noting that a quantitation could not be made in this case, as synthetic analogues of by-products were not available. Nonetheless, HPLC-MS peak areas can be considered proportional to concentrations and used for comparisons between the same species, provided that the spectrometer response reproducibility is checked. The latter control was accomplished during this work by performing periodical HPLC-MS runs on the herbicide solutions at the same concentration level (5 mg/L).

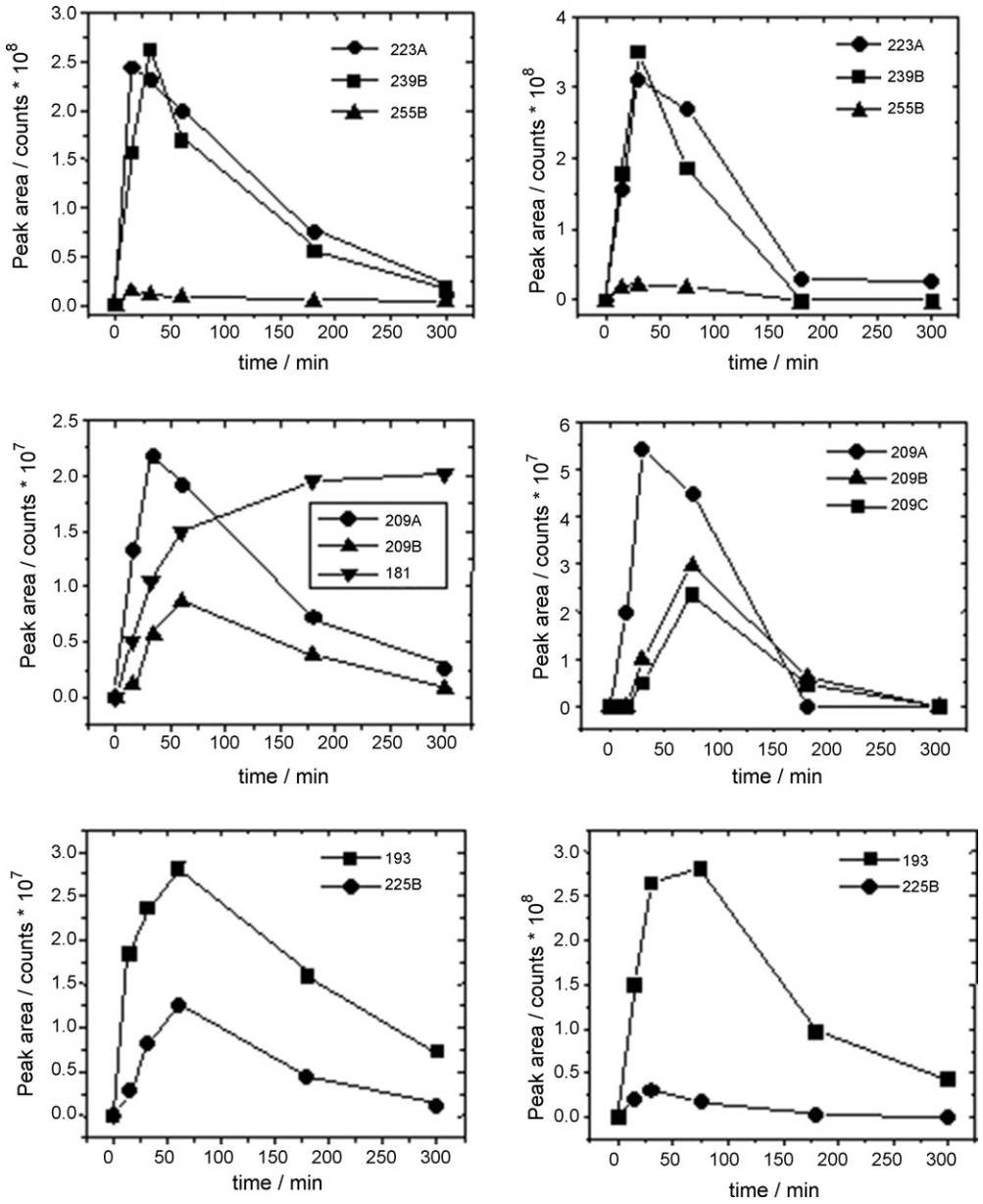

Fig. 4. Time course of the most representative by-products (SIM peak areas) obtained during isoproturon degradation by TiO_2/solar irradiation (left side) and EF process (right side).

Starting from data reported in Fig. 4, a global representation of the photocatalytic and of the EF process for isoproturon has been hypothesised and is reported in Schemes 1 and 2. Correlations between by-products have been established starting from structural information provided by LC–ESI-MS/MS. However, when MS/MS data were not conclusive, alternative structures had to be considered for a detected species (see, for examples, 239D, 225B and 255A and B).

In Schemes 1 and 2 a specific indication has been reported for species detected only during one of the two degradation processes.

Peak areas data suggest that isoproturon by-products exhibit a different behaviour according to their typology. Indeed, typical by-products arising from interaction with $^{\bullet}$OH radicals, i.e. mono- and multi-hydroxylated species (223, 239 and 255), appear as intermediates, their formation and further transformation rates being slightly higher in the case of the EF process, in accordance with data on the precursor. This effect is likely due to a higher concentration, during EF degradation, of $^{\bullet}$OH radicals.

Interestingly, single and multiple hydroxylations on the isopropyl group appear to be kinetically favoured in both processes. The absence of isomers 223C and D in the case of EF (whereas their peak areas are low in photocatalytically treated solutions) is likely due to their fast transformation into bi-hydroxylated products like 239C and D, that were indeed detected also in EF-treated solutions (see Scheme 1).

More remarkable differences between the two processes were observed on by-products arising from complex reactions, in particular for the demethylated derivative with *m/z* 193, whose maximum concentration was almost an order of magnitude higher in the case of EF. Consistently, its hydroxylated derivative 209B had a much lower peak concentration and 209C (involving hydroxylation on the dimethylamino group, like 193) was not detected at all in photocatalytically treated solutions.

Such differences were less pronounced in the case of 209A, whose generation involves demethylation/hydroxylation on the isopropylic side of isoproturon molecule.

Even more surprising is the already cited behaviour of species at *m/z* 181, a key intermediate in ISO ozonolysis [36]. This species appeared to be slowly formed during photocatalysis (see Fig. 4) but could not be detected in solutions subjected to EF degradation.

It is not clear if this finding arises from fast transformation of this compound in further by-products, too polar to be retained in the C8 column (like further hydroxylated compounds arising from species drawn at the bottom of Scheme 1), or if it suggests a peculiar reactivity on the isopropylic side of isoproturon molecule during photocatalysis.

In any case, the higher concentration of $^{\bullet}$OH radicals available during the EF process seems unable to explain the differences between the latter and photocatalysis for species like 193, 209 isomers and 181.

The potential need for adsorption of the isoproturon molecule (or its primary by-products) on immobilised TiO_2 during photocatalytical degradation could play a role.

3.3. Chlortoluron degradation pathway

The EF degradation rate for CHLT (see Fig. 2) appears to be comparable to the photocatalytical one (in the best conditions) [16]. However, remarkable differences in terms of by-product structures and kinetics were found, as shown in Table 1 and Fig. 5, respectively. The degradation pathways hypothesised for chlortoluron from these data are reported in Scheme 3.

The most remarkable finding is represented by the lower peak areas (and then concentrations), if any, obtained for several by-products during EF treatment.

In the case of mono-hydroxylated isomers, 229A and C were not detected in EF-treated CHLT solutions and the concentration of 229D was found to be lower with respect to photocatalysis.

Similarly, bi-hydroxylated 245D was not detected and species 245A, B and C were from two to five times less concentrated than the corresponding ones during photocatalytic degradations.

On the other hand, only EF-treated solutions provided evidence for the presence of a very polar species (retention time ca. 6.4 min) with *m/z* 261 (see Table 1 and Scheme 3). This *m/z* value is consistent with a triple hydroxylation of the CHLT molecule, although no information, other than an evidence for water loss, could be retrieved from the corresponding MS/MS spectrum, due to its very low concentration.

Moreover, the time evolution of SIM peak areas for the by-product at *m/z* 261 (not shown) indicates clearly its further transformation.

Although cross-correlations between species at different stages of hydroxylation (i.e. between isomers at *m/z* 229 and 245) are not possible, due to the lack of structural information, the data described so far suggest that multiple hydroxylations (double, triple, etc.) of CHLT are faster during EF. It can be hypothesised that such reactions lead ultimately to very polar products, not retained in the C18 column and then undetectable by ESI-MS/MS.

As a result, in spite of a similar decrease of the precursor concentration, the accumulation of species like mono- and bi-hydroxylated CHLT is higher, at the same time, during photocatalytic degradation.

By analogy with ISO, a different scenario can be hypothesised for CHLT by-products arising from more complex reactions. Among them, by-product at *m/z* 199, i.e. CHLT demethylated on the dimethylaminic side (see Scheme 3), showed a higher concentration during EF degradation.

It is worth noting that MS/MS data for this species excluded any correlation with CHLT demethylated on the benzene ring, which is indeed the precursor of the derivative at *m/z* 215 (see Scheme 2), detected only in photocatalytically treated CHLT solutions as an intermediate itself (data not shown).

A parallel discussion between CHLT and ISO can be made for the cited by-products. Indeed, demethylation on the dimethylaminic moiety is favoured by the EF treatment, like for ISO; the substitution of the benzene-linked methyl with a OH group (leading to by-product 215, corresponding to 209A for ISO) likely occurs both during photocatalytic and EF

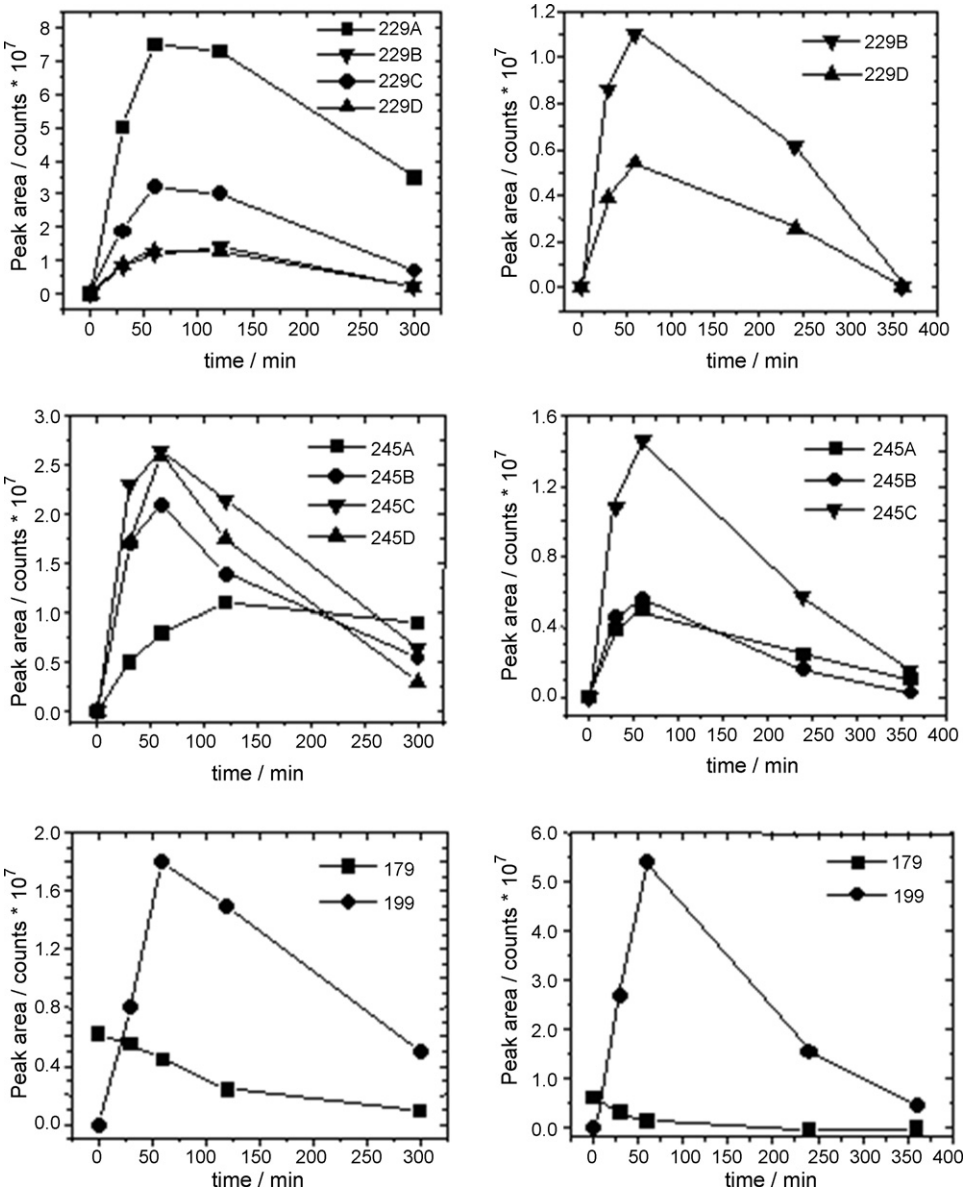

Fig. 5. Time course of the most representative by-products (SIM peak areas) obtained during chlortoluron degradation by TiO_2/solar irradiation photocatalysis (left side) and EF process (right side).

degradation of CHLT. However, fast further hydroxylation to polar, undetectable compounds (e.g. by-products with *m*/*z* 231), prevents its monitoring in the latter case.

On the other hand, the presence of a dechlorinated compound (*m*/*z* = 179) in both photocatalytically and EF-treated solutions is peculiar for CHLT.

As apparent from Fig. 5, the dechlorinated species was already detectable in the initial chlortoluron solution, before any degradation treatment. It could be then an impurity of the herbicide. Interestingly, this unexpected species was subjected to degradation both during photocatalytical and EF treatments, its half-life time being four times lower in the second case (see Fig. 5).

The presence of a by-product with *m*/*z* 195 in the case of photocatalysis, with peak areas having the typical profile of an intermediate (data not shown) indicated hydroxylation as the main degradation process for dechlorinated CHLT.

Consistently with hydroxylation on the herbicide itself, the further reaction towards very polar species was so fast, in the case of EF, that the by-product with *m*/*z* 195 could not be detected.

In principle, a parallel pathway for the formation of such a derivative, based on dechlorination/hydroxylation directly on a chlortoluron molecule (not on the impurity) cannot be excluded and is suggested by another interesting result arising from HPLC–ESI-MS analysis of EF-treated chlortoluron solutions.

Two highly retained (t_r of 39.5 and 40.6 min, respectively) isomeric species with *m*/*z* 247 were observed exclusively in the latter. The *m*/*z* ratio and the peculiar isotopic pattern suggested a bi-chlorinated structure for these compounds, whereas the presence of the diagnostic fragment at *m*/*z* 72 in the MS/MS spectrum indicated their correlation with CHLT.

Chlorination of the herbicide could be provoked only by reactive Cl atoms generated by the *in situ* dechlorination of

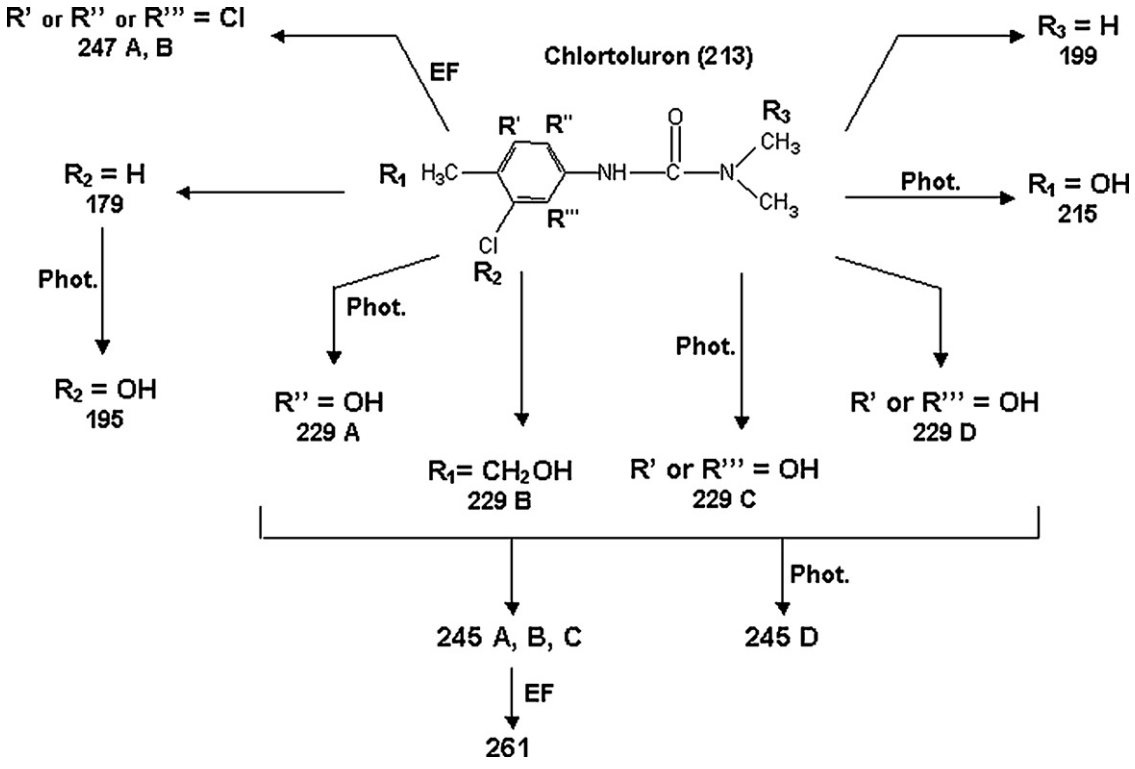

Scheme 3.

other chlortoluron molecules during the generation of by-product with *m/z* 195. Such a process, and then CHLT chlorination, is more significant, from a kinetic point of view, in the case of electro-Fenton degradation.

3.4. Chloroxuron degradation pathway

In the case of CHLOX no significant difference was observed between EF and photocatalysis both in the degradation kinetics of the precursor and in the nature and number of by-products. The time evolutions of HPLC–ESI-MS SIM peak areas for the most important among them are reported in Fig. 6. Some possible degradation pathways arising from these data are reported in Scheme 4.

In both cases direct hydroxylation of CHLOX generated three isomeric species ($m/z = 307$), depending on the aromatic ring interested by hydroxylation [16]. Actually the most retained isomer (classified as 307C) never reached significant concentrations, whereas the peak areas for the remaining ones suggested a higher concentration in the case of photocatalysis, as observed for mono-hydroxylated chlortoluron.

No evidence for further hydroxylation was obtained but the risk of a lack of chromatographic retention (and then of MS detection) for multi-hydroxylated molecules is probably higher in this case.

Demethylation was found to be a common feature of the two degradation processes also for CHLOX, as confirmed by the presence of a species (t_R ca. 31 min) with $m/z = 277$. Again, the reaction was faster for EF, since the maximum concentration of this compound was reached in a shorter time, compared to photocatalysis. On the other hand, its value was lower (see the relevant peak areas in Fig. 6).

This result is probably due to the presence of a peculiar reaction pathway for demethylated chloroxuron, leading to the substitution of the 4-chlorophenoxy moiety by a OH group (by-product with *m/z* 167, see Table 1 and Scheme 4).

Due to fast further transformation, in the case of EF the latter could be detected only at its maximum concentration, which was reached in a shorter time, compared to photocatalysis, thus confirming the correlation between species 277 and 167.

Interestingly, the substitution of the 4-chlorophenoxy moiety by a OH group was observed also on chloroxuron itself, leading to a species with *m/z* 181, already observed during isoproturon photocatalytic degradation. In this case the concentrations reached during EF degradation, although still lower than those relevant to photocatalysis, were high enough to enable the by-product detection.

The higher rate of further reaction due to EF treatment can be inferred also from the time evolution (see Fig. 6) of the by-product corresponding to a Cl/OH substitution (*m/z* 273), whose further hydroxylation lead to two chromatographically resolved isomeric species at $m/z = 289$, although their peak areas did not reach significant values.

It is worth noting that no dechlorinated product ($m/z = 257$) was observed for CHLOX. This finding, coupled to the presence of the dechlorinated/hydroxylated derivative, seems to confirm the hypothesis made for the generation of the corresponding derivative of chlortoluron (*m/z* 195).

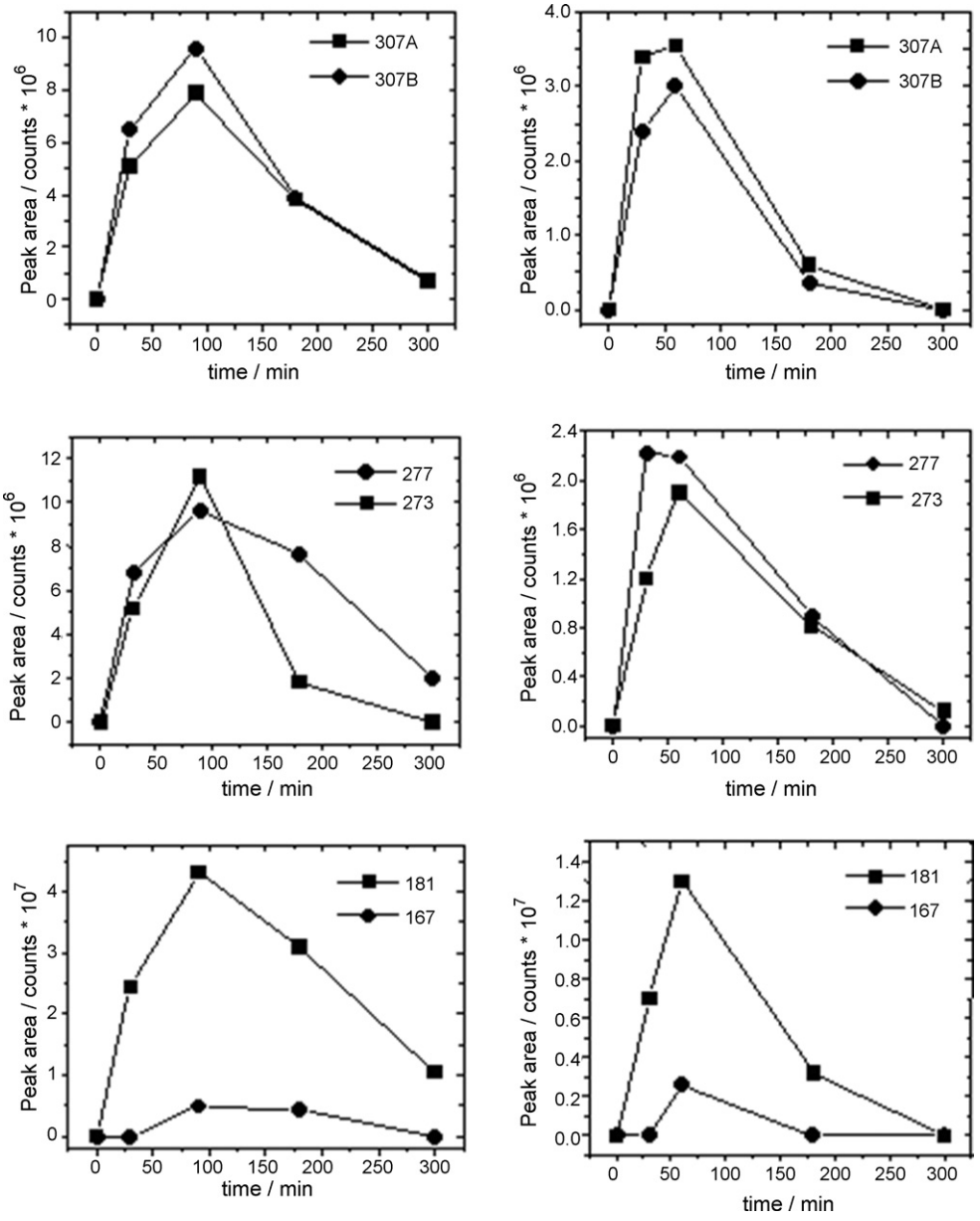

Fig. 6. Time course of the most representative by-products (SIM peak areas) obtained during chloroxuron degradation by TiO_2/solar irradiation photocatalysis (left side) and EF process (right side).

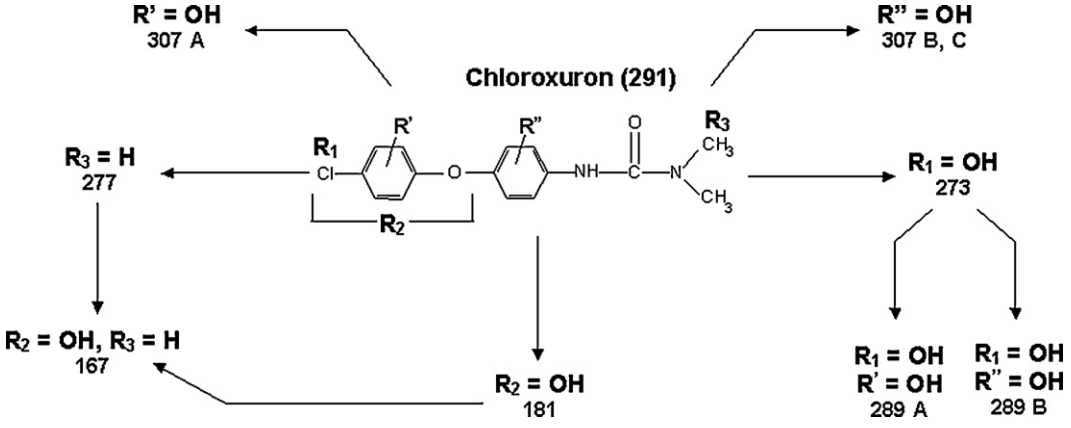

Scheme 4.

4. Conclusions

The first stages of the degradation pathways based on a electro-Fenton process for three phenyl-urea herbicides, isoproturon (ISO), chlortoluron (CHLT) and chloroxuron (CHLOX), could be investigated by reversed-phase (on C8 or C18 columns) HPLC–ESI-MS and MS/MS and compared to those relevant to the photocatalytic degradation on TiO_2 (immobilised in a PVDF film) under intense solar radiation.

Structural and quantitative cross-correlations were made between by-products generated: (i) in a specific degradation process; (ii) in the two processes under investigation for the same herbicide; (iii) from different herbicides during the same process.

As a result, general pathways for photocatalytic and electro-Fenton degradations could be hypothesised.

The most important reaction, common to all herbicides and to the two oxidation processes, was represented by hydroxylation on the aromatic ring(s), on the alkyl substituents (isopropyl and methyl for ISO and CHLT, respectively) and, to a minor extent, on a methyl group belonging to the dimethylaminic moiety. Hydroxylation could also occur by abstraction and substitution of an entire functional group (isopropyl, methyl or chlorophenoxyl for ISO, CHLT and CHLOX, respectively) or even of a Cl atom. The combination of such hydroxylation reactions usually led to several isomeric by-products of increasing polarity. Actually, species arising from two or, in some cases, three consecutive reactions could be separated and identified. Evidences for their further degradation were obtained indirectly but the corresponding by-products were too polar to be retained in the adopted HPLC columns and then characterised by ESI-MS, MS/MS.

A peculiar side reactivity of the investigated herbicides, common to the two oxidation process (and other AOPs as well), was represented by the demethylation on the dimethylaminic nitrogen, probably occurring via the already known hydroxylation of the corresponding methyl group, followed by oxidation to an aldehyde and subsequent release of formaldehyde. Evidences for subsequent hydroxylations on the demethylated herbicides were also found.

From a quantitative point of view, photocatalysis on TiO_2 and electro-Fenton in the best conditions (intense solar radiation and equimolar concentrations of herbicide and Fe^{3+}, respectively) provided similar degradation rates for the same herbicide. Chlorinated ones appeared more refractory than isoproturon.

Nonetheless, interesting differences were observed in terms of by-products persistency. Multiple consecutive hydroxylations appeared to be faster in the case of EF (especially on chlorinated herbicides), sometimes preventing intermediate by-products (like mono-hydroxylated) from being detected.

On the other hand, demethylated products reached higher or lower maximum concentrations during the EF treatment, compared to photocatalysis, according to the combination between generation and further hydroxylation kinetics.

Based on the obtained data, electro-Fenton appears to be a good alternative to photocatalysis on TiO_2 for the degradation of phenyl-urea herbicides.

Acknowledgements

Partial funding from University of Bari under Research Program *Progetti di Ricerca di Ateneo* is acknowledged. Mr. Simoncarlo Giacummo is gratefully acknowledged for his skilled technical help.

References

[1] R. Carabias-Martínez, E. Rodríguez-Gonzalo, M.E. Fernandez-Laespada, F.J. Sanchez-San Roman, J. Chromatogr. A 869 (2000) 471–480.
[2] R. Carabias-Martínez, E. Rodríguez-Gonzalo, E. Herrero-Hernandez, F.J. Sanchez-San Roman, M.G. Prado-Flores, J. Chromatogr. A 950 (2002) 157–166.
[3] R. Carabias-Martínez, E. Rodríguez-Gonzalo, M.E. Fernandez-Laespada, L. Calvo Seronero, F.J. Sanchez-San Roman, Water Res. 37 (2003) 928–938.
[4] P.R. Gogate, A.B. Pandit, Adv. Environ. Res. 8 (2004) 501–551.
[5] P.R. Gogate, A.B. Pandit, Adv. Environ. Res. 8 (2004) 553–597.
[6] M.R. Hoffmann, S.T. Martin, W. Choi, D.W. Bahnemann, Chem. Rev. 95 (1995) 69–96.
[7] S. Parra, J. Olivero, C. Pulgarin, Appl. Catal. B: Environ. 36 (2002) 75–85.
[8] K. Macounova, H. Krysova, J. Ludvik, J. Jirkovsky, J. Photochem. Photobiol. A: Chem. 156 (2003) 273–282.
[9] M. Haque, M. Muneer, J. Environ. Manage. 69 (2003) 169–176.
[10] M. Haque, M. Muneer, D.W. Bahnemann, Environ. Sci. Technol. 40 (2006) 4765–4770.
[11] S. Parra, J. Olivero, C. Pulgarin, Appl. Catal. B: Environ. 36 (2002) 131–144.
[12] S. Malato, J. Blanco, A. Vidal, D. Alarcon, M.I. Maldonado, J. Caceres, W. Gernjak, Sol. Energy 75 (2003) 329–336.
[13] S. Malato, J. Caceres, A.R. Fernandez-Alba, L. Pietra, M.D. Hernando, A. Aguera, J. Vial, Environ. Sci. Technol. 37 (2003) 2516–2524.
[14] I. Losito, A. Amorisco, F. Palmisano, P.G. Zambonin, Appl. Surf. Sci. 240 (2005) 180–188.
[15] A. Amorisco, I. Losito, F. Palmisano, P.G. Zambonin, Rapid Commun. Mass Spectrom. 19 (2005) 1507–1516.
[16] A. Amorisco, I. Losito, T. Carbonara, F. Palmisano, P.G. Zambonin, Rapid Commun. Mass Spectrom. 20 (2006) 1569–1576.
[17] J.J. Pignatello, Environ. Sci. Technol. 26 (1992) 944–951.
[18] Y. Sun, J.J. Pignatello, Environ. Sci. Technol. 27 (1993) 304–310.
[19] E. Brillas, E. Mur, J. Casado, J. Electrochem. Soc. 143 (1996) L49–L53.
[20] M.A. Oturan, J.J. Aaron, N. Oturan, J. Pinson, Pest. Sci. 55 (1999) 558–562.
[21] M.A. Oturan, J. Appl. Electrochem. 30 (2000) 475–482.
[22] B. Gözmen, M.A. Oturan, N. Oturan, O. Erbatur, Environ. Sci. Technol. 37 (2003) 3716–3723.
[23] E. Brillas, B. Boye, M.M. Dieng, J. Electrochem. Soc. 150 (2003) E148–E154.
[24] C. Flox, S. Ammar, C. Arias, E. Brillas, A.V. Vargas-Zavala, R. Abdelhedi, Appl. Catal. B: Environ. 67 (2006) 93–104.
[25] C. Flox, P.L. Cabot, F. Centellas, J.A. Garrido, R.M. Rodríguez, C. Arias, E. Brillas, Appl. Catal. B: Environ. 75 (2007) 17–28.
[26] E. Brillas, M.A. Banos, J.A. Garrido, Electrochim. Acta 48 (2003) 1697–1705.
[27] S. Irmak, H.I. Yavuz, O. Erbatur, Appl. Catal. B: Environ. 63 (2006) 243–248.
[28] A. Ventura, G. Jacquet, A. Bermond, V. Camel, Water Res. 36 (2002) 3517–3522.
[29] Y.B. Xie, X.Z. Li, Mater. Chem. Phys. 95 (2006) 39–50.

[30] E. Brillas, B. Boye, I. Sirés, J.A. Garrido, R.M. Rodrıguez, C. Arias, P.L. Cabot, C. Comninellis, Electrochim. Acta 49 (2004) 4487–4496.
[31] B. Boye, M.M. Dieng, E. Brillas, J. Electroanal. Chem. 557 (2003) 135–146.
[32] E. Brillas, J.C. Calpe, J. Casado, Water Res. 34 (2000) 2253–2262.
[33] M.A. Oturan, N. Oturan, C. Lahitte, S. Trevin, J. Electroanal. Chem. 507 (2001) 96–102.
[34] J. Anotai, M. Lub, P. Chewpreecha, Water Res. 40 (2006) 1841–1847.
[35] I. Sirés, N. Oturan, M.A. Oturan, R.M. Rodriguez, J.A. Garrido, E. Brillas, Electrochim. Acta 52 (2007) 5493–5503.
[36] G. Mascolo, A. Lopez, H. James, M. Fielding, Water Res. 35 (2001) 1695–1704.